Cement & Concrete Composites 41 (2013) 16–23

Contents lists available at SciVerse ScienceDirect

Cement & Concrete Composites

journal homepage: www.elsevier.com/locate/cemconcomp

Styrene–butadiene latex modified calcium aluminate cement mortar

Neven Ukrainczyk *, Anamarija Rogina

University of Zagreb, Faculty of Chemical Engineering and Technology, Marulićev trg 19, 10000 Zagreb, Croatia

ARTICLE INFO

Article history:
Received 27 May 2011
Received in revised form 22 April 2013
Accepted 25 April 2013
Available online 6 May 2013

Keywords:
Calcium aluminate cement
Hydration
Heat of hydration
Styrene–butadiene rubber (SBR)
Latex modified mortar
Mechanical properties
Rheology
Setting time

ABSTRACT

This paper investigates properties of calcium aluminate cement (CAC) mortar modified with the styrene–butadiene-rubber (SBR) latex. This material may be advantageously applied as a rapid repair mortar. Mortar specimens were prepared with constant water-to-cement mass ratio; polymer solid content of latex was varied from 0% to 9%, and Li_2CO_3 was investigated as an accelerator. Specimens were treated at different curing conditions: 1, 7 days and transformation of metastable hydration products at 70 °C. The heat of hydration evolution of mortar specimens was measured by means of a self adopted isoperibol calorimeter.

The measurement results indicate that SBR latex improves workability of fresh state mortar and retards nucleation and growth of hydration products. Due to polymer coagulation process and co-matrix formation permeability, stiffness and compressive strength decrease while adhesion strength to old concrete substrate, and flexural strength increase with amount of added latex.

© 2013 Elsevier Ltd. All rights reserved.

1. Introduction

Calcium aluminate cement (CAC) is a special cement with many specific properties [1–7]. Mainly due to fast hardening and excellent resistance to chemical attack, CAC is advantageously used for repair work of highways, airport's runways, internal and external building surfaces. Furthermore, the CAC is the preferred cement for polymer composites due to its high water to cement stoichiometric requirement that chemically bonds higher portion of water in the latex and thus enables higher degree of polymer coagulation. Setting and hardening of CAC is primarily due to the hydration of CA (cement notation: C = CaO, A = Al_2O_3, F = Fe_2O_3, S = SiO_2, H = H_2O), but other compounds also participate in the hardening process especially in long term strength development [1,7] and at higher temperatures of hydration. The CAC hydration is highly temperature dependent, yielding CAH_{10} as main products at temperatures less than 20 °C, C_2AH_8 [8] and AH_3 at temperatures about 30 °C, whereas C_3AH_6 and AH_3 at temperatures greater than 55 °C. CAH_{10} and C_2AH_8 are known to be metastable at ambient temperature and transform to more stable C_3AH_6 and AH_3 with consequent material porosity and permeability increment, and loss of strength. On the other hand, in the absence of sufficient water, these phases do not transform but dehydrate [8].

CAC harden rapidly with high early strengths even under low (near-freezing) temperatures [7], if protected from freezing prior to initial set. The hydration process of other types of cements (e.g. Portland cement, PC) is greatly slowed or even stopped at such low temperatures. Furthermore, CACs are favorably used in cryogenic areas, such as the loading docks of liquid–gas plants, because of the excellent thermal shock resistance [5]. The rapid hardening characteristic of CAC makes it suitable to put a cement based lining (e.g. floor or highway and bridge deck repair patch [9,10]) back in service within a few hours. The ultra-rapid setting CAC based materials, which set within a few minutes, can be readily obtained by a very small addition of Li salts [11,12]. The acceleration of the setting and hardening process generally results in a reduction of the ultimate strength [11,12].

Properties of cement-based materials can be improved by addition of a polymer admixture [13]. Upon hydration, the resulting hardened material contains a continuous, interconnected matrix of coagulated polymer particles which fill up pores in cement matrix and improve the bonding between aggregates and cement paste. As a result of this co-matrix formation, polymer modified mortars have low permeability, good freeze–thaw resistance, relatively higher flexural strength and adhesion strength to old concrete substrate, which allow those materials to be advantageously employed as repair materials for concrete buildings, concrete bridges, highway covering materials and waterproof materials [13]. Styrene–butadiene-rubber (SBR) latex modified mortars have been used on highway bridges in the US over the past 35 years. It is generally known that the polymer modified PC based material is more durable than the conventional one. In the last two decades, SBR latex-modified (PC) mortars have been widely used as

* Corresponding author. Tel.: +385 1 4597 323.
E-mail address: nukrainc@fkit.hr (N. Ukrainczyk).

0958-9465/$ - see front matter © 2013 Elsevier Ltd. All rights reserved.
http://dx.doi.org/10.1016/j.cemconcomp.2013.04.012

a repair materials for concrete and reinforced concrete structures because of their superior chemical as well as mechanical (e.g. frost attack, higher modulus of elasticity, higher tensile strength) resistance [13]. Polymer latex has been employed also in CAC based materials for making chemically resistant mortars, screeds and surface coatings [14]. Rubber latex modified CAC mortars are considerably more resistant than plain CAC mortars against dilute acid (pH >4), alkaline and oil (grease), and other chemical attack [14]. SBR is not resistant to oxidizing acids (e.g. nitric acid).

While the properties of different polymer latex-modified mortars based on ordinary (Portland) cements are widely reported in the literature, little is known on the polymer modification of the special CAC based materials. Systematic studies on the properties of the SBR modified CAC mortars are lacking in literature. Therefore, this paper presents the results on the effect of amount of added SBR polymer onto setting time, heat of hydration evolution, rheology, and physical and mechanical properties of a SBR latex modified CAC mortar.

2. Experimental

2.1. Materials

Commercial CAC (type ISTRA 40) was taken from a regular production of Calucem Pula, Croatia. The cement has the oxide mass fraction composition listed in Table 1. Physical properties of used cement are given in Table 2. The main compounds are CA and ferrite phase (C_4AF–C_6AF_2), with mayenite ($C_{12}A_7$), gehlenite (C_2AS) and β-C_2S as minor compounds. SBR latex with a 47% solid content, nonionic surfactant and antifoaming agent in the commercial composition was used. Mortars were prepared with distilled water and river sand with the size of 0–4.0 mm (100% passed 4 mm sieve). Analar grade Li_2CO_3 salt was used as an accelerator.

2.2. Specimen preparation

The sand-to-cement ratio for all specimens was 3 and (polymer solid)-cement ratios (p/c) were 0%, 3%, 6% and 9%. The amount of water in the latex emulsion was taken into account in the overall water-to-cement mass ratio which is fixed at 0.450. Li_2CO_3 accelerator was dissolved in freshly deionised water prior to mixing with cement with a mass fraction of 0.0045% relative to cement weight.

In order to reduce the amount of entrained air the following mixing method was used. First, cement and sand were mixed together in a standard laboratory planetary mixer (following ASTM C305-80) for 1 min at speed of 140 rpm. Then, the water was added into the mix and mixing process was continued for 2 min at the same speed. At last, latex was added and everything was mixed for another 2 min. Fresh mixtures were cast into prismatic molds ($40 \times 40 \times 160$ mm) and vibrated. Specimens were cured in mold for 24 h at 20 °C and 95% of relative humidity. In order to investigate properties of hardened CAC mortars with morphologically different hydration products, the aimed specimens were obtained according to a designed experimental hydration program shown in Table 3. The specimens were hydrated at 20 °C to obtain CAH_{10} as main hydration product. After 7 days of hydration (Table 3), the metatable hydration products were transformed to the stable ones (nominally C_3AH_6 and AH_3) by additional heating of the specimens (sealed in plastic bags) at 70 °C in a thermostated water bath for 24 h.

2.3. Experimental methods

The consistency (fluidity) of the fresh state mortar was tested using the standard flow table test according to EN 1015-3. The test procedure involved placing the mold (60 mm in height, internal diameter: base 100 mm – top 70 mm) in the center of the flow table. A period of 15 s is allowed to elapse before the mold is removed, the table is jolted 15 times at a rate of one jolt per second. The mean diameter of the spread mortar is recorded.

Apparent density and air entrapment of mortars were determined following ASTM C185-08. The mortars were compacted (vibrated) into a measure of known volume and weighed. The air content is calculated from the measured apparent density of the mortar, the known densities of the constituents, and the mixture proportions. CAC and sand densities are determined according to the ASTM C 188-89.

Bending and compression test of hardened mortars were done as per EN 1015-11. The bending tests were performed on $40 \times 40 \times 160$ mm prisms, while the compression tests were carried out on two pieces of original prisms for each specimen. The standard molds were filled by placing on a vibrating table.

The open porosity was obtained from the measurements of the dry weight (W_D), the water saturated weight (W_{Sat}) and the sample volume (on broken halves of standard prisms by Archimedes method, W_{Arch}), according to the following equation:

$$P_{OPEN} = \frac{W_{Sat} - W_D}{W_{Arch}} \quad (1)$$

Drying of samples was achieved by using a vacuum pump for 1 day (at 0.5 mbar). Drying of samples by heating is not used because of the well known effect of the transformation reactions [1] that significantly modified the pore microstructure of CAC based material.

Ultrasonic modulus (E) for each specimen was determined by the following equations:

$$E\ (\mathrm{GPa}) = \frac{v^2 \rho}{K} \quad (2)$$

$$K = \frac{(1-v)}{(1+v)(1-2v)} \quad (3)$$

where ρ is the sample density, (g cm^{-3}), v the velocity of ultrasonic pulse propagation through the specimen (160 mm long), (km s^{-1}), v is the Poisson's coefficient.

The velocity of ultrasonic pulse propagation through the specimen was measured by TICO Proceq Testing Instruments with time resolution of 0.1 μs, voltage impulse of 1 kV, pulse repetition of 3 s^{-1} and frequency of 54 kHz.

Determination of adhesive strength of hardened mortar on concrete substrates was done as per EN 1015-12. This test method involves determining the maximum tensile stress applied by a direct load at right angles to the surface of the mortar. The substrate used was a PC based concrete panels with dimensions $550 \times 150 \times 50$ mm with a maximum aggregate size of 8 mm. The concrete panels were wood floated to provide a suitable surface and are more than 28 days old when testing was undertaken.

Table 1
Chemical composition (mass%) of investigated CAC.

CaO	Al_2O_3	Fe_2O_3	FeO	SiO_2	TiO_2	MgO	SO_3	Na_2O	K_2O	Sum
37.95	38.00	13.11	2.77	4.23	1.59	0.65	0.20	0.14	0.18	98.82

Table 2
Physical properties of investigated CAC.

>90 μm (%)	Blaine ($cm^2\ g^{-1}$)	Specific gravity ($g\ cm^{-3}$)	Setting time (min)		Standard consistency (%)
			Initial	Final	
3.70	3308	3.20	300	329	24.0

Table 3
Specimen curing conditions after demolding.

Curing series	Curing conditions after demolding (in mold for 24 h at 100% RH and 20 °C)
1 d	0 h (tested immediately)
7 d	6 days at 20 °C 40% RH
14 d	13 days at 20 °C 40% RH
Trans70c	6 days at 20 °C 40% RH, transformed 24 h at 70 °C

The fresh mortar was spread to the substrate using notched steel trowel to achieve a thickness of 10 mm ± 1 mm. For the first 24 h the test specimens are stored in an airtight polyethylene bag (to maintain high relative humidity) at a temperature of 20 °C. After that, the specimens are stored in 50% RH and 20 °C for the next 6 days (corresponding to the sample 7 d in Table 2). After 7 days of hydration (Table 3), the metastable hydration products were transformed to the stable ones (nominaly C_3AH_6 and AH_3) by additional heating of the specimens at 70 °C and 100% RH for 24 h. The test is then performed using the pull off instrument (DYNA Z16 pull-off tester by Proceq) to apply a tensile force until failure occurs.

The water absorption coefficient due to capillary action of hardened mortar specimens was measured according to EN 1015-18. Broken sides of a standard mortar prism were immersed to a depth of 5–10 mm in water and the amount of absorbed water was determined with time.

The heat of hydration evolution was measured by means of a self adopted laboratory isoperibolic calorimeter. The employed calorimeter consists of an insulating container (composed mainly of styrofoam cups with stoppers), temperature sensor, and thermostated bath, as shown in Fig. 1. The temperature change in the calorimeter is measured by K-type thermocouples (wire thickness of 0.2 mm). Temperature is stored every 15 s by a data logger PICO Logger TC-08 (Pico Technology Ltd., UK: 20 bits, eight channels, voltage resolution 1 μV) connected to PC with *PicoLog for Windows* software. The thermocouples were calibrated using high accuracy Pt 100 probe. Thermocouple cold junction is held at room temperature and sensed by a precision thermistor in good thermal contact with the input connectors (on thermal block) of the measuring instrument. In order to assure good cold junction compensation, a change of its temperature is kept as low as possible.

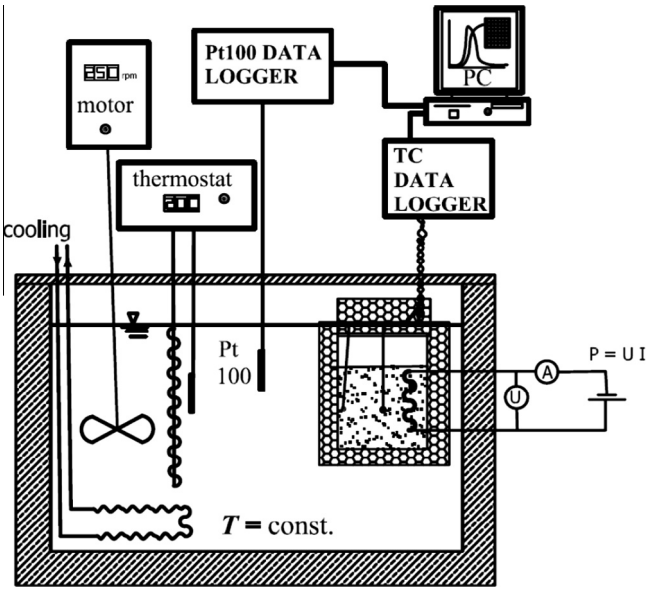

Fig. 1. Scheme of the calorimetric measurement set-up.

The cement, sand and appropriate amount of water was left to reach thermal equilibrium (overnight) before manual mixing in the calorimeter. The calorimeter (Fig. 1) is quantitatively filled with a mortar sample (prepared with 40 g of cement for all mortar mixtures tested with experimental variables shown in Table 4) sealed with styrofoam stopper and immersed in temperature controlled water bath $T = 20$ °C (±0.03 °C). Dimensions of the calorimeter are: inner diameter $D = 50$ mm, height $H = 45$ mm and thickness of the stytrofoam isolation $d = 4.5$ mm. Two thermocouples were placed in the calorimeter. One thermocouple measuring end was placed at the mass center of the sample, i.e. through the axis at half thickness of the sample. This was done by fixing thin (1.3 mm) wooden support at the axis of the container. The second thermocouple was placed at the inner surface (mortar–calorimeter interface) of the calorimeter.

The evolved heat of hydration per gram of cement ($J\ g^{-1}$) was calculated by employing the lumped-parameter heat transfer model:

$$Q(t) = \frac{C_p}{m}(\Delta T(t) + \beta \int_0^t \Delta T(t)) \quad (4)$$

where C_p is the effective heat capacity of the calorimeter, ($J\ °C^{-1}$), β the cooling constant of the calorimeter, (h^{-1}), m the cement mass, (g)

The following calorimeter parameters were estimated: the heat loss constant (α, isoperibolic [$J\ °C^{-1}\ h^{-1}$]), the cooling constant (β, h^{-1}), and the effective heat capacity (C_p, [$J\ °C^{-1}$]). The calibrations were done by applying a known voltage to a known electrical resistance (thin constantan wire) embedded in a block of hardened cement paste. The heat loss from the calorimeter to the surrounding was obtained from a steady state condition measurement (the voltage was applied until the steady state was achieved). In steady state the heat loss equals the heating power dissipating on the embedded resistance wire. The cooling constant of the calorimeter was obtained from the transient temperature response after switching off the Joules heat in the calorimeter. The cooling constant (β) was estimated by nonlinear regression ('fitting') of the exponential solution of Newton's law of cooling to the transient

Table 4
Experimental variables and sample notation for calorimetric measurements.

Sample notation	p/c (%)	Li_2CO_3 (%)
0	0	0
3	3	0
6	6	0
9	9	0
6LC	6	0.0045
9LC	9	0.0045

experimental results. Calorimeter parameters were experimentally obtained for each test mortar mixture.

The presented results are the average of at least three specimens in flexure, six specimens in compression, six specimens in bond strength and three specimens for all other tests.

3. Results and discussion

3.1. Calorimeter

The calorimetric measurements were conducted in a manner to obtain realistic temperature rise of the mortars that mimic the temperature rise of the specimens cured in the $40 \times 40 \times 160$ mm standard molds. This was achieved by an appropriate thickness of the insulating material, geometry of the cell while ensuring enough mass of sample and low mortar temperature gradients during measurement (i.e. low Biot number [15]). All the mortar mixtures for calorimetric measurements were prepared with 40 g of cement. Both the calculated value of the Biot number, $Bi = 0.04$, and the measured maximal temperature difference across mortar samples during the calorimetric measurements, $\Delta T < 0.6$ K justified the usage of the lumped-parameter model (Eq. (1)) for the calculation of the heat of hydration evolution. Results of the temperature rise of mortar samples during hydration in the isoperibolic calorimeter are given in Fig. 2. Low temperature rise is observed during the induction period due to a small and constant rate of heat generation, about 1 J h^{-1} g^{-1} for the mortars without Li_2CO_3 and 3 J h^{-1} g^{-1} for mortars with Li_2CO_3 accelerator. Induction period is followed by the onset of the accelerated stage of reaction due to massive precipitation of hydration products. The maximum of heat generation is reached in only few hours after the onset of the accelerated stage and amounts up to about 125 J h^{-1} g^{-1}.

The rapid hydration and the resulting heat evolution allows an accurate determination of both the induction time t_0 and the time t_{max} of the maximum of temperature evolution peak. Indeed, though less traditional and indirect, preferable techniques for measuring setting time are isothermal calorimetry, temperature rise, and solution conductivity measurements [12,16]. In this paper times of initial, t_0 and final, t_f sets for experimental series on transition metals were established from the obtained time–temperature curves. Initial set is acquired from the intersection of two straight lines [17]: one fitted through the induction period of the curve and the other fitted through the inflection point of the rising slope of the main peak. The final set was approximated as the point of maximal heat generation. Table 5 lists the results of the analysis of calorimetric temperature rise curves: times of initial, t_0 and final, t_f sets, the inflection point (*i.p.* [h]) of the rising slope (*slope*) of the main peak.

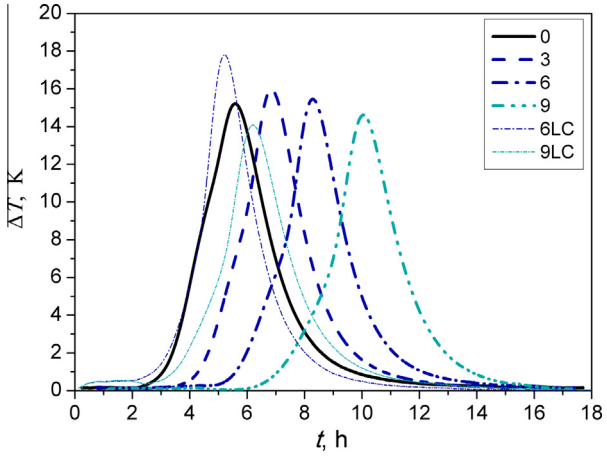

Fig. 2. Temperature rise of mortar samples during calorimetric measurements: effect of polymer content and addition of Li_2CO_3 (sample notation and experimental variables are listed in Table 4).

Table 5
Analysis of calorimetric temperature rise curves: times of initial, t_0 [h] and final, t_{end} (h) sets, the inflection point (*i.p.* [h]) of the rising slope (*slope* (K h^{-1})) of the main peak.

Sample notation	t_0 (h)	t_{end} (h)	*i.p.* (h)	*slope* (K h^{-1})
0	3.23	5.59	4.02	7.36
3	4.38	6.80	5.12	5.71
6	5.56	8.29	6.47	4.28
9	6.98	10.02	8.08	2.99
6LC	3.06	5.23	3.92	5.74
9LC	3.40	6.16	3.95	3.10

Both the influence of the polymer addition and the addition of Li_2CO_3 accelerator are investigated by calorimetric measurements. The results show that SBR latex significantly retards the CAC hydration kinetics. Both the nucleation and the subsequent growth of hydration products are retarded. The retardation is more pronounced with rising of the polymer content. The observed slower crystallization and growth of hydration products may be interpreted in terms of the cement hydration inhibiting effect of the surfactants contained in latexes [13] as well as blocking of the reactive cement sites by coagulation of a low permeable polymeric matrix.

Effect of the addition of Li_2CO_3 accelerator is investigated on mixtures that contain 6% and 9% of polymer. From the results presented in Fig. 2 and Table 5 it can be seen that very small addition of Li_2CO_3 (0.0045% relative to weight of cement) significantly accelerates the hydration. By comparison of the two hydration curves (Fig. 2 and Table 5) one can observe the combined effect of polymer and Li_2CO_3 addition. The polymer retards both the nucleation and growth of hydration products. It is interesting that the Li_2CO_3 accelerates the nucleation period much more effectively than the further growth of the hydration products (i.e. rising slope of the main hydration peak). This agrees well with the fact that the effect of a low permeable polymeric matrix on hydration kinetics is higher with higher degree of coagulation (i.e. degree of hydration). During CAC hydration reactions free water content is decreasing due to chemically combining in hydration products which results in the coagulation of the SBR polymer.

Fig. 3 presents the calculated heat of hydration evolution curves of prepared CAC mortar samples. The results show the effect of polymer content and addition of Li_2CO_3 on the CAC hydration. Heat evolution curves provide an approximation on a relative amount of achieved hydration degree [7,18]. It can be concluded that the relative hydration degree after 24 h has a lowering tendency with the amount of polymer addition. This may be attributed to the inhibiting effect of the surfactants contained in latexes as well as to the formation of the protective SBR coatings that hinder crystallization and growth of the hydration products. From the cumulative heat curves (Fig. 3) it can be observed that when Li_2CO_3 is added, the total heat measured for different polymer additions, is lower than in the mixtures without Li_2CO_3. This is consistent with the literature results obtained on cement pastes [12,17].

3.2. Fresh state properties

3.2.1. Consistency

The result on fresh state mortars consistency with different latex solid contents (p/c) are summarized in Table 6. Specimens mixed with constant water-to-cement ratio show increment in

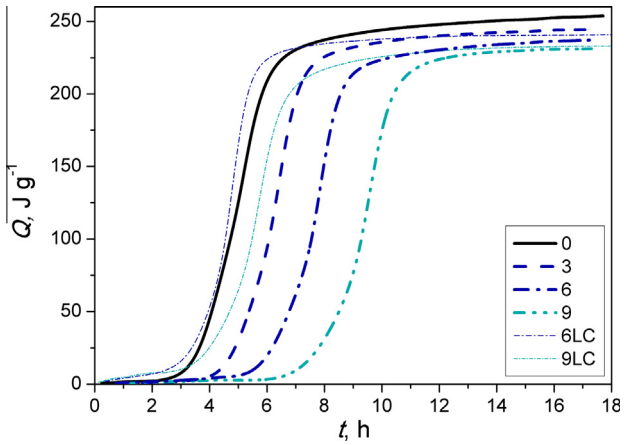

Fig. 3. Heat of hydration evolution of mortars with different polymer content and addition of Li_2CO_3 accelerator (sample notation and experimental variables are listed in Table 4).

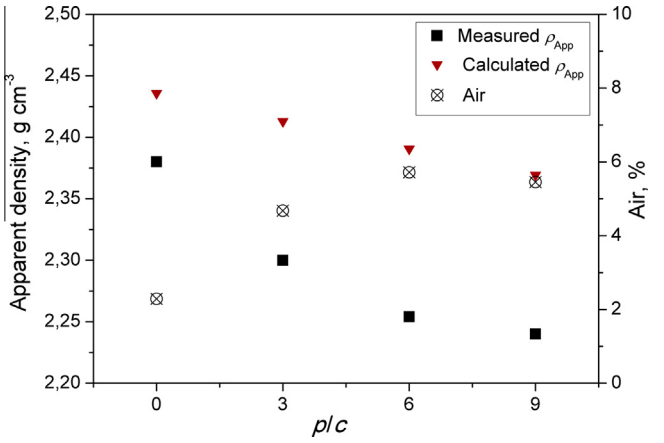

Fig. 4. Apparent density and air content of prepared fresh mortars with different polymer contents (p/c).

workability by increasing the p/c ratio. The inclusion of polymer latex improves mortar workability, due to the 'ball bearing' action of polymer particles, the entrained air and the dispersing effect of surfactants [13]. This enables a reduction in water-to-cement ratio that influence positively on porosity, compressive and flexural strength of hardened mortar: reducing porosity and increasing flexural and compressive strength [13].

3.2.2. Densities and air content

Fig. 4 shows results on apparent densities and air content of prepared fresh mortars with different polymer contents. The air content is calculated from the measured density of mortars, and known densities of the constituents (Table 2, latex density is 1.02 g cm^{-3}, sand 2.85 g cm^{-3}), and the mixture proportions.

3.2.3. Air entrainment

Addition of latex for preparing mortars usually entrains a considerable quantity of air compared to non-modified mortars. This increase in air entrainment is due to an effect of the emulsifying and stabilizing surfactants in polymer latex. Commercial latexes for cement modification usually contain some antifoaming agents that considerably decrease the air entrainment. Entrained air should be optimized. A disadvantage of air entrainment is a reduction in strength, but the positive side is improvement in workability (consistency, due to 'ball bearing' action) and durability [13]. Entrained air forms closed-types spherically-shaped pores, sizes of 10–300 μm, which improve cohesion and workability of the mixture. The closed pores contribute to a reduction in transport of aggressive ions and gases, and to a better resistance to frost.

3.3. Hardened state properties

3.3.1. Compressive and flexural strength

The effect of polymer content (p/c) and curing conditions on compressive strength and flexural strength of CAC mortar specimens is depicted in Figs. 5 and 6, respectively. Latex modified mortar show a decrease in the compressive strength but noticeable increase in the flexural strengths with polymer addition when compared to reference (unmodified) mortars.

Specimens of all curing series show the same trend, higher latex content reduces compressive strength due to a lower mechanical capacity of SBR polymer regarding to mortar. Test results show that mortars of series 1 d, 7 d and 14 d have an increasing trend for strength (flexural and compressive) with hydration time, which can be attributed to higher degree of hydration as well as polymer coagulation process. The lowest compressive strength values are achieved for the fully transformed mortar series (Trans70C in Table 2), due to the well known transformation process that results in the increase of porosity.

The addition of SBR latex increases the flexural strength of mortars. This improvement in tensile strength may be attributed to the high tensile strength of the coagulated polymer and an overall improvement in cement-sand bond. Moreover, from the mechanical point of view, polymer latexes bridge microcracks in the latex-modified mortar and concrete under stress by the formation of polymer films, which prevents crack propagation. For curing series 1 d, 7 d and 14 d the highest polymer content increases the reference flexural strength by 18%, 31% and 29%, respectively. For the transformed specimens the reduction of flexural strength amounts only 8%. For curing series 1 d, 7 d and 14 d the highest polymer content reduces the reference compressive strength by 42%, 34%

Table 6
Consistency of fresh state LMM for each p/c ratio.

p/c (%)	Consistency, mm
0	150
3	155
6	170
9	195

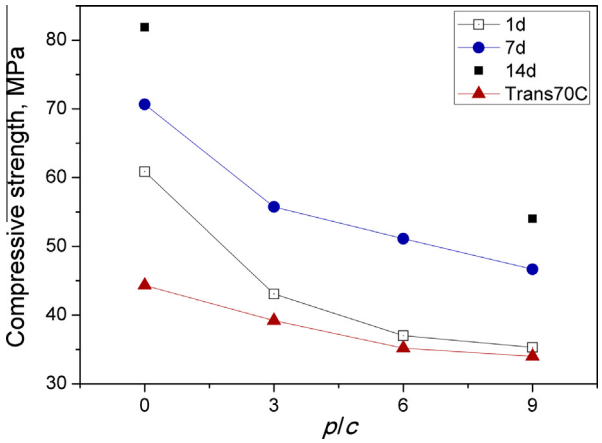

Fig. 5. Effect of polymer content (p/c) and curing conditions on compressive strength of CAC mortar specimens.

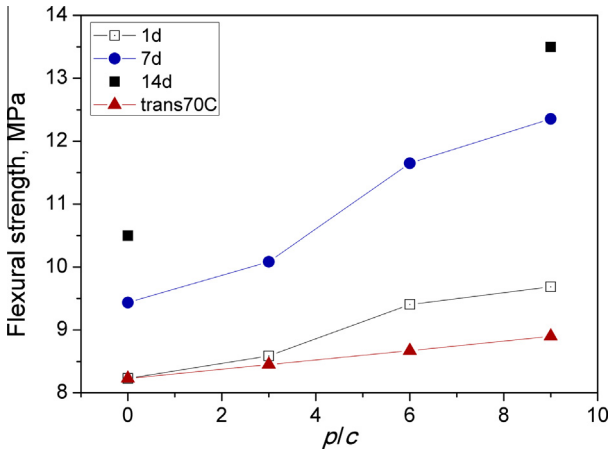

Fig. 6. Effect of polymer content (p/c) and curing conditions on flexural strength of CAC mortar specimens.

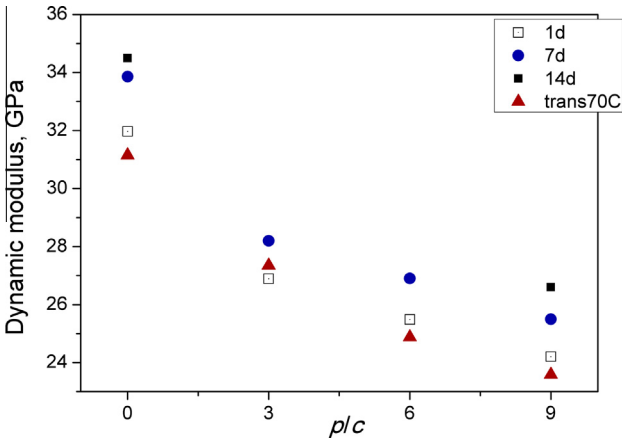

Fig. 7. Dynamic modulus of mortar specimens for different polymer contents (p/c) and curing conditions.

and 34%, respectively. For the transformed specimens the reduction of compressive strength amounts 23%. Interestingly, from the results obtained it can be concluded that both the positive effect of gain in flexural strength and the negative effect of reduction in compressive strength are much lower for the transformed material regarding to the metastable state series. This can be explained by the change in the microstructure (with transformation reactions) and/or modification of polymer properties with thermal treatments. Here, it has to be noted that high temperature lead to the weakening of the bonding between mortar matrix and SBR polymer due to the deterioration or decomposition of polymer [13]. The temperature effect on strength of SBR modified CAC mortars was not investigated separately in this paper, due to the temperature sensitivity of the transformation reactions. To separate both temperature effects, on SBR and on CAC hydration, the transformation of the metastable hydration products to the fully stable ones needs to be performed below near room temperatures. However, transformation reactions at such temperatures are known to take a very long time (decades).

3.3.2. Dynamic modulus

Dynamic modulus (or stiffness) of mortar specimens for different polymer contents and different curing conditions is shown in Fig. 7. For the calculation of the dynamic (ultrasonic) modulus of mortar specimens (E) (Eqs. (2) and (3) in Section 2.3) the Poisson's coefficient was taken to be $\nu = 0.2$ for all specimens tested [19]. Indeed, one can expect a decrease of the Poisson's coefficient with age [14], while the effect of polymer addition can be disregarded [13,20]. However, the primarily aim of the analysis in Fig. 7 is to see the effect of the polymer content on the dynamic modulus within the same curing conditions. As expected the stiffness of the prepared mortar specimens decreases with latex content increment. This decrease in stiffness is attributed to a lower polymer stiffness in regard to plain (reference) mortar stiffness. An increment of the dynamic modulus with hydration time for metastable mortar series 1 d, 7 d and 14 d (1, 7 and 14 days) is a result of the higher advancement of the hydration reaction. The lowest dynamic modulus values are achieved for the fully transformed mortar series (Trans70C in Table 2), as a result of the well known transformation process that results in the increase of porosity. However, as discussed above, for more precise comparison of the trends among the different curing conditions one should also include an increase of dynamic modulus due to a possible decrease of the Poisson's ratio with hydration time [14].

3.3.3. Adhesion

Results of adhesion in tension of latex-modified CAC mortars to ordinary (Portland cement) mortar are depict in Fig. 8. All adhesive failures occurred at the mortar–concrete interface. It is clear that the adhesion of latex modified mortars tends to increase with raising the polymer content. The increase in adhesion is attributed to the high adhesion of polymer. The increase in adhesion may be explained by a mechanical interlocking of coagulated SBR ensured by porous and rough surface of the substrate concrete panel. This may be further enhanced by a chemical interaction of the surfactant located on polymer–concrete interphase. The surfactant acts as a compatibilizer between organic (SBR) and inorganic (concrete and mortar) phase. Indeed, the use of latex-modified pastes and mortars as bonding agents for PC mortars to existing mortar (or concrete) substrates is a widespread practice. The bond strength results obtained for CAC mortars are comparable to the results on PC based materials tested by other researchers [7,13,21,22].

3.3.4. Open porosity

The effect of polymer content and curing conditions on open porosity of CAC mortar specimens is presented in Fig. 9. A reduction of the open porosity with polymer addition can be observed for all curing series. This can be attributed to the filling of pores by coagulated SBR polymer as well as to the higher air entrainment stimulated by polymers and surfactants in the latex. Both coagu-

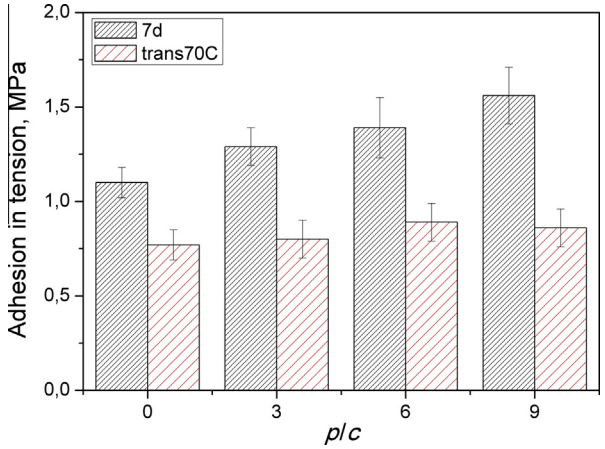

Fig. 8. Adhesion in tension of latex-modified CAC mortars to ordinary (Portland cement) concrete. All adhesive failures are at mortar–concrete interface.

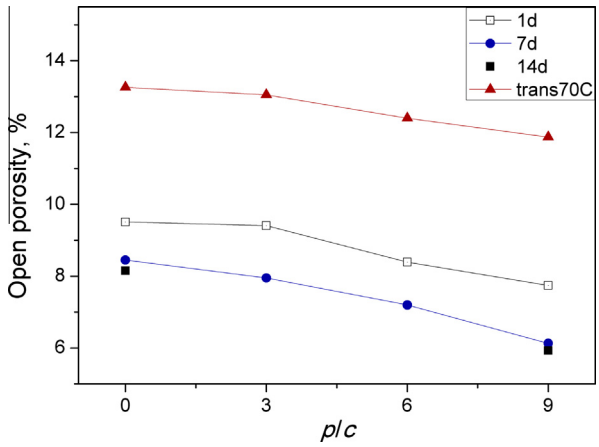

Fig. 9. Effect of polymer content (p/c) and curing conditions on open porosity of CAC mortar specimens.

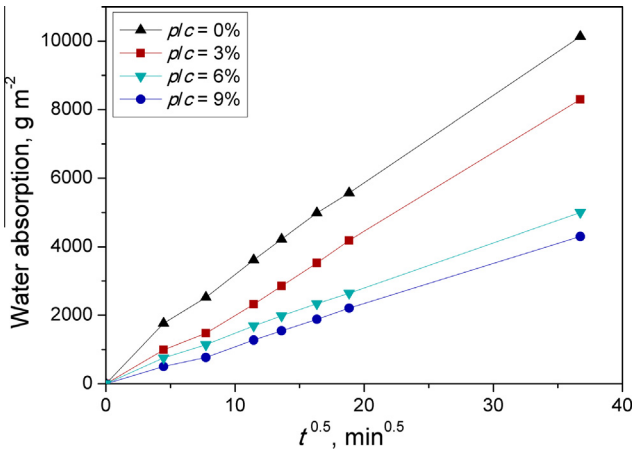

Fig. 11. Effect of polymer content on the capillary water absorption of the transformed specimens (trans70C, Table 3).

lated SBR and air bubbles contribute to the depercolation (i.e. closed porosity) of the pore system. A decrease in open porosity with hydration time for metastable mortar series 1 d, 7 d and 14 d (Fig. 9) is a result of the higher degree of depercolation of pores due to the advancement of the hydration reaction and higher degree of SBR coagulation. The fully transformed mortar series (Trans70C in Table 2) exhibit the highest values for the open porosity, due to the well known transformation process that results in the increase of porosity. Although the total porosity was not investigated in this paper, it is worth nothing that its trends with curing conditions are expected to be inversely related to the results of compressive strengths (Fig. 5).

3.3.5. Capillary water absorption

The variation of the water uptake with time due to capillary action of hardened mortar specimens 7 d and Trans70C (Table 3) is shown on Figs. 10 and 11, respectively. The calculated sorption coefficients are given in Table 7. All of the transformed samples exhibit drastically higher capillary water absorption in comparison to the samples that are composed mainly of the metastable hydration products (Figs 10 and 11, Table 7). This expected effect is a result of the transformation process that increases the porosity of the CAC based materials. The latex modified mortar reduced drastically the water absorption of both the metastable and the transformed specimens and showed the decreasing tendency with the amount

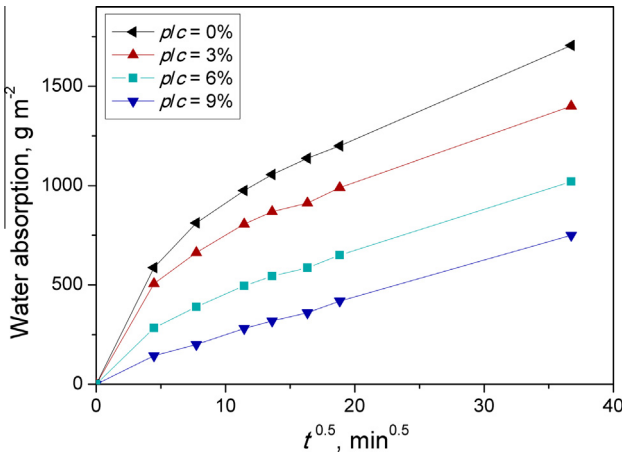

Fig. 10. Effect of the polymer content on the capillary water absorption of the metastable specimens (curing series 7 d in Table 3).

Table 7
Results of the sorption coefficient, S (g m^{-2} min$^{-0.5}$).

p/c (%)	Curing	
	7 d	Trans70c
0	46.5	261
3	38.1	228
6	27.8	132
9	20.4	118

of SBR addition. This reduction in the water absorption can be ascribed to the coagulated polymer filling of the pores, lowering of the open porosity (Fig. 9), and bridging of the microcracks propagating inside the matrix.

The nonlinear behavior observed in Fig. 10 may be attributed to the change in the mortar microstructure with time as the water penetrates the sample. Indeed, after re-wetting of the dried sample capillary actions induce change in the pore microstructure and the cement particles can be re-activated again upon cement water interaction In this nonlinear case, the sorption coefficient was calculated (according to EN 1015-18) as the slope from the intercept to the last reading (i.e. 24 h). Interestingly, the non-linear behavior diminishes with the amount of the added polymer (p/c). This can be interpreted by the covering of the active cement particles with the inert polymer co-matrix as well as by the stabilization effect of the polymer onto the change in the pore microstructure induced by capillary actions. Moreover, the capillary absorption of the fully transformed specimens showed a reasonably linear behavior.

4. Conclusion

The effects of polymer modification of CAC mortars were studied by fixing the water-to-cement ratio. The following can be concluded. SBR latex significantly retards the CAC hydration kinetics. Both the nucleation and the subsequent growth of hydration products are retarded. The retardation is more pronounced with higher addition of the polymer content. A very small addition of Li_2CO_3 (0.0045% relative to weight of cement) successfully accelerates the hydration of polymer modified CAC mortar.

Latex modified mortar show a decrease in the compressive strength but noticeable increase in the flexural strengths with polymer addition when compared to unmodified mortar. The lowest compressive strength values are achieved for the fully transformed mortar series, due to the well known transformation

process in CAC based materials that results in the increase of porosity. Stiffness of the prepared mortar specimens decreases with latex content increment. Adhesion of latex modified mortars to the concrete substrate tends to increase with raising the polymer content.

A reduction of the open porosity with polymer addition can be observed for all curing series. This can be attributed to the filling of pores by coagulated SBR polymer as well as to the higher air entrainment stimulated by polymers and surfactants in the latex. Both coagulated SBR and air bubbles contribute to the depercolation of the pore system. The latex modified mortar reduce drastically the water absorption of both the metastable and the transformed specimens, the more so with the higher amount of SBR addition.

Acknowledgements

The authors acknowledge support from the Croatian Ministry of Science, Education and Sports under Project's No. 125-1252970-2983 'Development of Hydration Process Model', and wish to thank LGM firm (Zagreb, Croatia) for providing SBR latex samples, and Calucem d.o.o. (Pula, Croatia) for providing cement samples.

References

[1] Bensted J. Calcium aluminate cements. In: Structure and performance of cement. London: Bensted J, Barnes P; 2002.
[2] Mangabhai RJ, Scrivener KL, editors. Calcium aluminate cements. Proceedings of the Centenary Conference, Avignon: 30 June–2 July, 2008. Fentiman CH, IHS BRE Press; 2008, EP94.
[3] Mangabhai RJ, Glasser FP, editors. Calcium aluminate cements. In: Proc. Int. Conf. on CAC. London: IOM Communications; 2001.
[4] Mangabhai RJ, editor. Calcium aluminate cements. London: Chapman & Hall; 1990.
[5] Scrivener KL, Cabiron JL, Letourneux R. High-performance concretes from calcium aluminate cements. Cem Concr Res 1999;29(8):1215–23.
[6] Ukrainczyk N, Matusinović T. Thermal properties of hydrating calcium aluminate cement pastes. Cem Concr Res 2010;40(1):128–36.
[7] Ukrainczyk N. Kinetic modeling of calcium aluminate cement hydration. Chem Eng Sci 2010;65(20):5605–14.
[8] Ukrainczyk N, Matusinovic T, Kurajica S, Zimmermann B, Sipusic J. Dehydration of a layered double hydroxide-C_2AH_8. Thermochim Acta 2007;464(1–2):7–15.
[9] The Concrete Society. Technical Report 46: Calcium aluminate cements in construction – a re-assessment. Camberley: The Concrete Society; 1997.
[10] Justnes H. Rapid repair of airfield runway in cold weather using CAC mortar. In: Mangabhai RJ and Scrivener KL, editors. Calcium Aluminate Cements. Proceedings of the Centenary Conference. Avignon: 30 June–2 July 2008. Fentiman CH, IHS BRE Press; 2008. p. 365–72.
[11] Matusinović T, Vrbos N, Čurlin D. Lithium salts in rapid setting high-alumina cement materials. Ind Eng Chem Res 1993;33(11):2795–800.
[12] Ukrainczyk N, Vrbos N, Sipusic J. Influence of metal-chloride salts on calcium aluminate cement hydration. Adv Cem Res 2012;24(5):249–62.
[13] Ohama Y. Handbook of polymer-modified concrete and mortars. New Jersey, USA: Noyes Publications; 1995.
[14] Robson TD. High-alumina cements and concrete. New York: John Wiley & Sons; 1962.
[15] DeWitt, Bergman, Lavine. Fundamentals of heat and mass transfer. New York: John Wiley & Sons; 2007.
[16] Stegemann JA, Buenfeld NR. Neural network prediction of setting of calcium aluminate cements containing additions. In: Mangabhai RJ, Glasser FP, editors. Proc. Int. Conf. on CAC. Edinburgh, UK; 2001. p. 267–79.
[17] Bushnell-Watson SM, Sharp JH. The effect of temperature upon the setting behaviour of refractory calcium aluminate cement. Cem Concr Res 1986;16(6):875–84.
[18] Gosselin C, Gallucci E, Scrivener K. Influence of self heating and Li_2SO_4 addition on the microstructural development of calcium aluminate cement. Cem Concr Res 2010;40(10):1555–70.
[19] Barluenga G, Hernandez-Olivares F. SBR latex modified mortar rheology and mechanical behaviour. Cem Concr Res 2004;34(3):527–35.
[20] Bureau L, Alliche A, Pilvin Ph, Pascal S. Mechanical characterization of a styrene–butadiene modified mortar. Mater Sci Eng 2001;A308(1–2):233–40.
[21] Ramezanianpour AA, Parhizkar T. Performance of repair mortars in hot weather conditions. In: Proceeding of the 7th International Conference on Inspection, Appraisal, Repairs and Maintenance of Building and Structures. Nottingham, UK; 2001. p. 541–7.
[22] Belaidi ASE, Azzouz L, Kenai S, Benabed B, Menadi B. Properties and durability of repair material of damaged structures in hot environment. International Conference on Construction and Building Technology, Kuala Lumpur, vol. A (33); 2008. p. 365–74.